Theoretical Design of n-Type Organic Semiconducting Materials Containing Thiazole and Oxazole Frameworks

ARTICLE *in* THE JOURNAL OF PHYSICAL CHEMISTRY A · APRIL 2014

Impact Factor: 2.69 · DOI: 10.1021/jp500899k · Source: PubMed

3 AUTHORS, INCLUDING:

Truong Tai
University of Leuven
65 PUBLICATIONS **507** CITATIONS
SEE PROFILE

Minh Tho Nguyen
University of Leuven
748 PUBLICATIONS **10,856** CITATIONS
SEE PROFILE

THE JOURNAL OF PHYSICAL CHEMISTRY A

Article

pubs.acs.org/JPCA

Theoretical Design of n-Type Organic Semiconducting Materials Containing Thiazole and Oxazole Frameworks

Vu Thi Thu Huong, Truong Ba Tai, and Minh Tho Nguyen*

Department of Chemistry, University of Leuven, B-3001 Leuven, Belgium

Supporting Information

ABSTRACT: The characteristics of molecular structure and charge transport of some new n-type organic semiconductors containing thiazole **1a**−**6a** and oxazole **1b**−**6b** frameworks and trifluoromethylphenyl as terminal groups were predicted using density functional theory (DFT) methods. The energy levels of HOMO and LUMO of these compounds are decreased when thiophene and furan units are replaced by thiazole and oxazole units, respectively. The same trend was observed when benzo[1,2-*d*:4,5-*d*′]bisthiazole groups were replaced with benzo[1,2-*d*:4,5-*d*′]bisthiazole-4,8-diones. The reorganization energies for electron of compounds are computed in a range of 0.21−0.37 eV, which is comparable to the value of 0.25 eV of well-known n-type semiconductors such as perfluoropentacene. Some important trends can be pointed out as follows: (i) replacing the core thiazolothiazole unit of compounds **1a** and **2a** by the larger core benzo[1,2-*d*:4,5-*d*′]bisthiazole units of **3a** and **4a** decreases both reorganization energies for electron (λ_e); (ii) the λ_e values of compounds containing thiazole **2a**, **4a**, and **6a** are smaller than those of compounds containing thiophene **1a**, **3a**, and **5a**, respectively; (iii) there is no clear trend when replacing benzene rings of compounds **3a** and **4a** by quinone rings of **5a** and **6a**. The λ_e values of **5** and **6** are only somewhat larger. The same trend is also found for compounds containing oxazole **1b**−**6b**. The intermolecular charge transports in solid state of these compounds mainly occur among molecules in the same molecular layer, whereas intermolecular interactions between molecules in different molecular layers are very small. Generally, beside some experimentally reported molecules **1a**−**4a**, the remaining molecules designed here are good candidates for n-type organic semiconducting materials with small reorganization energies for electron and low energy levels of LUMO.

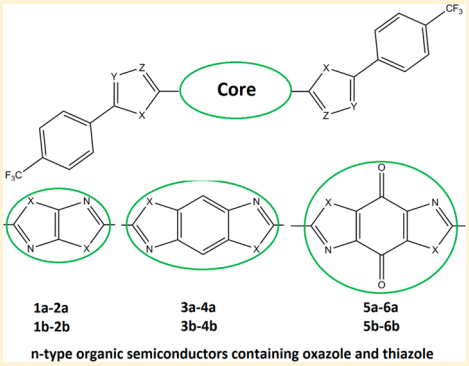

n-type organic semiconductors containing oxazole and thiazole

1. INTRODUCTION

The π-conjugated organic semiconducting materials are of considerable current interest owing to their key role in the fabrication of high performance organic electronic devices such as organic field-effect transistors (OFETs), organic light emitting diodes (OLEDs), and organic photovoltaic cells (OPVs).[1−3]. A good organic semiconductor is required to exhibit high ambient stability and efficient charge transport characteristics. In this context, some p-type organic semiconductors such as pentacene and rubrene[4,5] have emerged as promising materials with high FET mobility that exceeds that of amorphous silicon field effect transistors (FETs, α-Si:H, mobility ∼1.0 $cm^2\ V^{-1}\ s^{-1}$).[6] However, similarly effective n-type organic semiconductors are rather scarce although they play a primordial role in fabricating complete and complementary circuits.[7,8] As a consequence, the search for n-type semiconductors constitutes a stimulating and actual challenge.

Despite the fact that numerous π-conjugated organic semiconducting materials were experimentally investigated over the past four decades, an understanding about the relationship between molecular structure and charge transport properties of materials remains quite limited. One of the most important advantages of organic semiconductors is that their molecular structures can easily be modified by either combining several different molecular units to form cooligomers and copolymers or substituting different functional groups into parent compounds.[9,10] This allows us to design tailor-made materials with considerably improved physicochemical properties. However, we are also facing many challenges as the performance of organic electronic devices not only depends on the nature of materials but also is affected by several different factors such as the methods of production of device, purity of materials, type of electrodes, and so on. Fortunately, these complex effects can be avoided in theoretical investigations using quantum chemical computations that are now able to provide us with realistic structure−property correlations.

In this context, we set out in the present work to design and investigate the characteristics of molecular structure and charge transport properties of some new n-type organic semiconductors containing thiazole **1a**−**6a** and oxazole **1b**−**6b** frameworks (Figure 1) and having trifluoromethylphenyls as terminal groups. Thiazole and its derivatives such as benzo[1,2-*d*:4,5-*d*′]bisthiazole, bithiazole, and thiazolothiazole are well-known as electron-accepting planar heterocyclic compounds

Received: January 25, 2014
Revised: April 5, 2014
Published: April 10, 2014

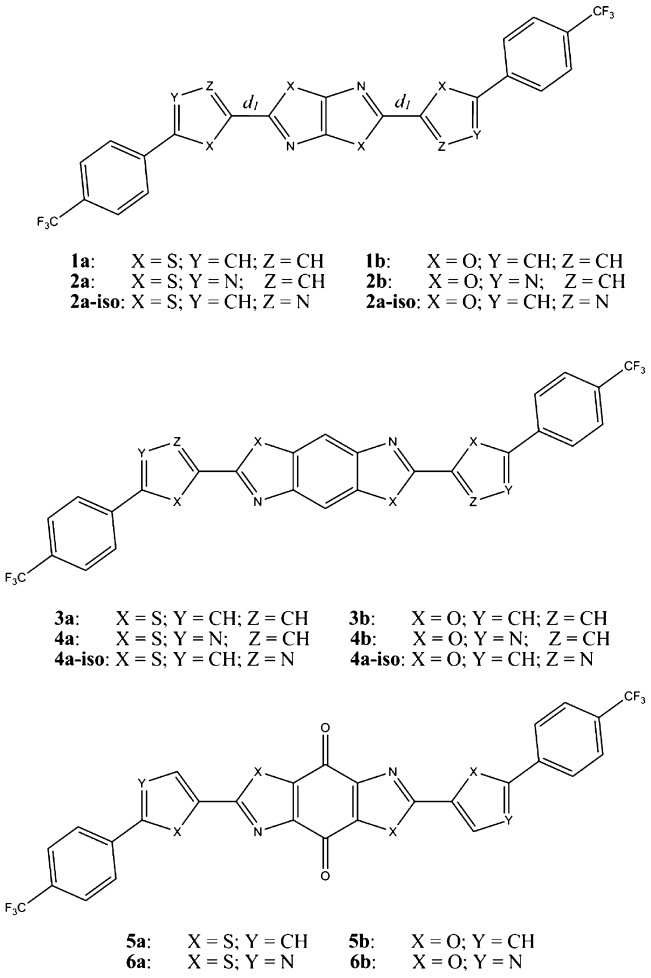

Figure 1. Chemical structures of molecules **1a**−**6a** and **1b**−**6b**.

that are widely used in both n-type and p-type organic semiconductors.[11,12] Introduction of these moieties into novel organic semiconductors based on thiophene is expected to downshift the energy levels of their HOMO and LUMO, which results in better ambient stability. In addition, the lowering of the LUMO levels of n-type semiconductors tends to decrease the energy barrier between their |LUMO| and work function of gold electrode (∼5.1 eV) that subsequently improves their transport characteristics. In fact, the syntheses of some compounds such as **1a**−**4a** shown in Figure 1 were previously reported.[13] However, the effect of molecular structures on their FET mobility has not been well understood yet due to the different conditions used in fabricating FET devices. For instance, the FET mobility of compound **2a** was reported to be 0.64 $cm^2\ V^{-1}\ s^{-1}$ by Mamada et al.[14] which is higher than the value of 0.30 $cm^2\ V^{-1}\ s^{-1}$ of **1a** reported by Ando et al.,[15] but lower than the value of 1.2 $cm^2\ V^{-1}\ s^{-1}$ of **1a** reported in ref 16. Although the compounds **2a** and **2a-iso** were found to have similar electrochemical properties and crystal structures, the FET characteristics of bottom contact devices made from these materials turn out to be much different from each other. While **2a** revealed FET mobility of 0.64 $cm^2\ V^{-1}\ s^{-1}$, that of **2a-iso** is very low (0.3×10^{-3} $cm^2\ V^{-1}\ s^{-1}$).[14] Similar observations were also found for compounds **4a** and **4b-iso**.[17] Thus, a theoretical investigation on these compounds provides us with more insight into these interesting phenomena.

In order to design new n-type semiconductors, we replace benzo[1,2-*d*:4,5-*d*′]bisthiazole moieties in compounds **3a** and **4a** by benzo[1,2-*d*:4,5-*d*′]bisthiazole-4,8-dione units to form compounds **5a** and **6a**, respectively, whose levels of LUMO are expected to be decreased. Finally, replacement of thiazole units in **1a**−**6a** by oxazole counterparts also leads to different n-type semiconducting materials **1b**−**6b**.

2. COMPUTATIONAL METHODS

2.1. Charge Transport Properties. In order to probe the charge transport properties, the hopping model is used.[18−23] In this model, the hole and electron carriers can be jumped between the adjacent molecules of the organic crystals. The rate of charge hopping (K) can be evaluated by using the Marcus−Hush equation (eq 1):[24]

$$K = (t^2/\hbar)\exp(-\lambda/4k_BT)\sqrt{\pi/\lambda k_BT} \quad (1)$$

where t is the transfer integral between two adjacent molecules, λ the reorganization energy, k_B the Boltzmann constant, and T the working temperature (being 298 K in our calculations). Accordingly to eq 1, a high rate of charge hopping K is attained when the transfer integral (t) between two molecules is high, and the monomers have low reorganization energy (λ).

The transfer integral is defined by eq 2,[25−27]

$$t = \langle \varphi_i^{0,\text{site1}} | F | \varphi_j^{0,\text{site2}} \rangle \quad (2)$$

where $\phi_i^{0,\text{site1}}$ and $\phi_j^{0,\text{site2}}$ present the HOMO (or LUMO) of isolated molecules 1 and 2, respectively. F is the Fock operator ($F = SC\varepsilon C^{-1}$) of the dimer with a density matrix from non-interacting dimer, where S is the intermolecular overlap matrix, and C and ε are the molecular orbital coefficients and energies from one-step diagonalization without iteration, respectively. The transfer integral for hole (t_h) is calculated as half of the energy difference between the HOMO and HOMO−1 of the dimer, while the transfer integral for electron (t_e) is the half of the energy difference between the LUMO and LUMO+1 of the dimer. These orbital energy levels are obtained using density functional theory (DFT) with the PW91 functional[28,29] in conjunction with the 6-31G(d,p) basis set. This approach has been proven to be suitable and effective in calculations of the transfer integrals of many organic compounds.[30−38]

2.2. Reduction and Oxidization Potentials in Solution. The reduction and oxidization potentials of compounds in solution are calculated by using a protocol recently developed by Davis and Fry.[39] First, optimizations of geometries and calculations of harmonic vibrational frequencies of each compound in the neutral, anionic, and cationic charge states are performed at the B3LYP/6-31+G(d) level. Their single point electronic energies are obtained using a larger basis set, B3LYP/6-311++G(2df,2p). Addition of a set of diffuse functions (++) in the basis set is necessary to describe the structures of the ions involved in the evaluation. The SMD/IEF-PCM solvation model[40] is used to probe the solvent effects. These methods were proven to be effective to obtain the reduction and oxidation potentials of PHA compounds in solution.[39,41] In the present case, we use acetonitrile (CH_3CN) as the working solvent.

The absolute potentials at 298 K are obtained using eq 3,

$$E^{298}_{\text{Abs}} = E^{298}_{\text{calc}} - 0.03766 \quad (3)$$

where E^{298}_{calc} is calculated from the difference in free energy (G) at 298 K between the couples neutral/cation and anion/

dx.doi.org/10.1021/jp500899k | J. Phys. Chem. A 2014, 118, 3335−3343

Table 1. Oxidation and Reduction Potentials (eV) and Energy Levels of HOMO and LUMO (eV) of Compounds Considered in Acetonitrile Solution (B3LYP/6-311++G(2df,2p)//B3LYP/6-31+G(d) Using the SMD/IEF-PCM Solvation Model)

	$E_{1/2}^{red}$	$E_{1/2}^{oxd}$	LUMO	HOMO	gap		$E_{1/2}^{red}$	$E_{1/2}^{oxd}$	LUMO	HOMO	gap
1a	−1.62 (−1.88)[a]	1.01	−3.18	−5.81	2.62	**1b**	−1.78	0.92	−3.02	−5.72	2.70
2a	−1.43 (−1.48)[a]	1.28	−3.37	−5.81	2.71	**2b**	−1.56	1.21	−3.24	−6.01	2.77
3a	−1.57 (−1.80)[a]	1.16	−3.23	−5.96	2.73	**3b**	−1.87	1.08	−2.93	−5.88	2.95
4a	−1.49 (−1.39)[a]	1.37	−3.31	−6.17	2.86	**4b**	−1.70	1.37	−3.10	−6.17	3.07
5a	−0.60	1.42	−4.20	−6.22	2.02	**5b**	−0.53	1.41	−4.27	−6.21	1.94
6a	−0.54	1.71	−4.26	−6.51	2.25	**6b**	−0.52	1.67	−4.32	−6.47	2.15

[a]The values in parentheses were obtained from available experimental reports (**1a**, ref 15; **2a**, ref 14; **3a**, ref 17; **4a**, ref 17).

neutral. The value of 0.03766 accounts to small thermal correction for a free electron at 298 K.[42]

The reduction potential is predicted in CH_3CN solution for the ferrocene−ferrocenium (Fc/Fc^+) pair, and the standard redox couples are calculated by using expressions 4 and 5:

$$\text{reduction:} \quad E_{1/2}{}^{298} = 1.056E^{298}{}_{Abs} - 4.90 \tag{4}$$

$$\text{oxidation:} \quad E_{1/2}{}^{298} = 0.932E^{298}{}_{Abs} - 3.94 \tag{5}$$

2.3. Electronic Structure Calculations. Optimizations of the relevant geometries and calculations of their harmonic vibrational frequencies are fully performed using DFT methods. The functionals including the hybrid B3LYP[43−45] are used in conjunction with the 6-31G(d,p), 6-31+G(d,p), and 6-311++G(2df,2p) basis sets.[46,47] For open-shell systems including the cations and anions, the unrestricted formalism (UB3LYP) is used. This functional has again been demonstrated to be reliable in predicting geometrical parameters and charge transport properties of many π-conjugated systems.[35−37] For each species considered, the corresponding neutral, anionic, and cationic states are characterized. All electronic structure calculations are carried out using the Gaussian 09[48] suite of programs.

3. RESULTS AND DISCUSSION

3.1. Geometries of Compounds Considered. Geometry optimizations and calculations of harmonic vibrational frequencies of all compounds examined are performed using the hybrid B3LYP functional in conjunction with the polarized 6-31G(d,p) basis set. Reliable geometries and charge transport properties of the organic semiconductors have been obtained using this approach in many previous studies.[49−54] The chemical structures of all compounds considered are shown in Figure 1, whereas their shapes and coordinates are given in the Supporting Information.

A good agreement between our computed geometries and the available experimental parameters can be noted. For instance, the computed C−C distance (d_1) between the thiazolethiazole core and two thiophene moieties of **1a** is 1.440 Å, which is close to the experimental values of 1.439−1.443 Å.[15] Similarly, the computed C−C bonding length (d_1) of 1.440 Å between the thiazolethiazole core and two thiazole moieties of **2a** also agrees well with the experimental values of 1.444−1.449 Å.[14] Interestingly, our predictions show that compounds **2a**, **4a**, and **6a** containing thiazole have planar geometries, whereas compounds **1a**, **3a**, and **5a** containing thiophene are slightly twisted out of the molecular plane. In agreement with experimental results,[14] the compound **2a** has a planar structure, while compound **2a-iso** is twisted. Interestingly, all compounds **1b**−**6b** are found to have planar structures.

3.2. Electrochemical Properties. Frontier molecular orbitals (FMO) are primordial descriptors in probing organic semiconductors. For n-type organic semiconductors, earlier studies showed that their LUMO level should be in the range of −3.0 to −4.5 eV. This not only makes the materials kinetically more stable with respect to ambient oxidation conditions but also reduces energy barriers between the n-type semiconductors and work function of gold electrode (~5.1 eV in vacuum). Although some other metals such as aluminum, magnesium, and so on were also used as electrodes with lower work functions, they are not preferred because of their lower stability in ambient conditions.

Since experimental measurements are usually carried out in solution, theoretical predictions performed using continuum solvent models allow us to obtain more comparable and useful results. In this work, reduction and oxidation potentials and subsequently energy levels of frontier orbitals of the molecules are calculated using the SMD/IEF-PCM solvent model.[55] Our computed results summarized in Table 1 are in good agreement with the available experimental values. The computed reduction potentials of **2a** and **4a** are −1.43 eV and −1.49 eV, which are close to the experimental values of −1.48 eV[14] and −1.39 eV,[17] respectively. The $E^{1/2}{}_{red}$ values of compounds **1a** and **3a** are predicted to be −1.62 eV and −1.57 eV, respectively, which are somewhat higher than the experimental values of −1.88 eV[15] and −1.80 eV.[17]

Interestingly, the HOMO and LUMO values listed in Table 1 reveal that of all compounds are in a range of −3.18 to −4.26 eV, which turns out to be very good for n-type organic semiconductors. More importantly, some variable trends for the energy levels of their HOMO and LUMO emerged as follows:

(i) First, replacement of thiophene units by thiazole units results in decreasing energy levels of both HOMO and LUMO. The HOMO and LUMO values of **2a**, **4a**, and **6a** are systematically lower than those of **1a**, **3a**, and **5a**, respectively.

(ii) Second, small differences in the HOMO and LUMO levels of energy are observed when the core thiazolelothiazole units in **1a** and **2a** are replaced by benzo[1,2-*d*:4,5-*d*′]bisthiazole units in **3a** and **4a**, respectively.

(iii) Our predictions consistently reveal that replacement of benzo[1,2-*d*:4,5-*d*′]bisthiazoles in **3a** and **4a** by benzo-[1,2-*d*:4,5-*d*′]bisthiazole-4,8-diones in **5a** and **6a** consid-

dx.doi.org/10.1021/jp500899k | J. Phys. Chem. A 2014, 118, 3335−3343

erably reduces their HOMO and LUMO energy levels. The LUMO energy levels of **5a** and **6a** are located at −4.20 and −4.26 eV, respectively, which are very good for n-type organic semiconductors.

(iv) Finally, the effect of dione on LUMO energy levels of oxazole analogues is larger than on that of thiazole analogues. The LUMO energy levels of compounds **5b** and **6b** are systemically lower than those of compounds **5a** and **6a**, respectively. The LUMO values of **1b**−**4b** are higher than those of **1a**−**4a**, respectively.

Similar trends can be found for the compounds **1b**−**6b** containing oxazole units. The HOMO and LUMO values of **2b**, **4a**, and **6b** are in fact lower than those of **1b**, **3b**, and **5b**, respectively.

3.3. Reorganization Energy. The reorganization energy is a key parameter in the evaluation of both electron and hole mobilities of a molecule. It is defined as the sum of geometrical relaxation energies when the species goes from the neutral state geometry to a charged state geometry, and vice versa. A description of these terms on a potential energy surface is schematically shown in Figure 2. Accordingly, a molecule

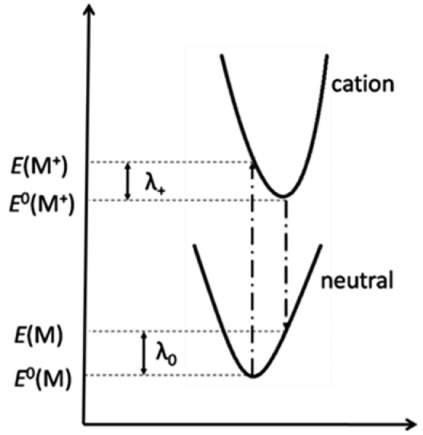

Figure 2. A schematic definition of the reorganization energy for hole.

exhibits high charge mobilities when it has low reorganization energies that can be defined as follows:

$$\lambda_h = \lambda_0 + \lambda^+ = [E(M) - E^0(M)] + [E(M^+) - E^0(M^+)] \quad (6)$$

$$\lambda_e = \lambda_0 + \lambda^- = [E(M) - E^0(M)] + [E(M^-) - E^0(M^-)] \quad (7)$$

where λ_h and λ_e are reorganization energies for hole and electron, respectively; $E(M^+)$ and $E(M^-)$ are the total energies of the cationic and anionic states with the optimized geometries of the neutral ground state, respectively; $E(M)$ is the total energy of the neutral state with the optimized geometries of the cationic species (for eq 6) and of the anionic species (for eq 7); and $E^0(M)$, $E^0(M^+)$, and $E^0(M^-)$ are the total energies of the neutral, cationic, and anionic ground state species, respectively.

Although the values of reorganization energies for hole (λ_h) of all compounds considered are close to their λ_e values, they are rather large as compared to the typical values of p-type semiconductors previously reported.[35,51] Thus, these molecules cannot be suggested for p-type organic semiconductors.

The reorganization energies for electron of compounds **1a**−**6a** are computed to be in a range of 0.21−0.34 eV. These values are comparable to that of 0.25 eV of perfluoropentacene (**PFPEN**)[35] which is one of the best known n-type organic semiconductors. Additionally, **1a** was also found to be a good candidate for n-type organic semiconductors with a high FET mobility of 1.2 $cm^2\ V^{-1}\ s^{-1}$. Because **1a** is characterized by the largest λ_e value as compared to those of the remaining molecules, the compounds designed above are thus expected to exhibit good charge transport character as well.

More importantly, some remarkable observations can also be pointed out. First, replacement of a core thiazolothiazole unit of compounds **1a** and **2a** by larger core units of **3a** and **4a** decreases their reorganization energies for electron (λ_e). Second, the λ_e values of compounds containing thiazole **2a**, **4a**, and **6a** are smaller than those of compounds containing thiophene **1a**, **3a**, and **5a**, respectively. However, no clear trend emerges when replacing benzene rings of compounds **3a** and **4a** by quinone rings of compounds **5a** and **6a**. The λ_e values of **5** and **6** are only marginally larger.

The computed results listed in Table 2 also point out that the λ_e values of compounds **2a-iso** and **4a-iso** are much larger than those of their isomers **2a** and **4a**, respectively (λ_e(**2a**) = 0.25 eV, λ_e(**2a-iso**) = 0.37 eV, λ_e(**4a**) = 0.21 eV, λ_e(**4a-iso**) = 0.31 eV). This is consistent with the previous experimental result that the FET mobility of **2a** is much higher than that of **2a-iso** (**2a**, μ = 0.64 $cm^2\ V^{-1}\ s^{-1}$, and **2a-iso**, $\mu = 0.3 \times 10^{-3}$ $cm^2\ V^{-1}\ s^{-1}$).[14] Our computed results show that, following addition of one excess electron, all anions **2a**, **2a-iso**, **4a**, and **4a-iso** have planar geometries (see Table S3, Supporting Information). While the neutrals **2a** and **4a** also exhibit planar structures, the **2a-iso** and **4a-iso** have twisted geometries. The large differences in geometrical structures between neutral and anionic states are the main reason for the much larger λ_e values of **2a-iso** and **4a-iso** as compared to those of **2a** and **4a**, respectively.

Table 2. Reorganization Energies for Electron and Hole of Compounds Obtained at the B3LYP/6-31G(d,p) Level of Theory

compd	λ_e (eV)	λ_h (eV)	compd	λ_e (eV)	λ_h (eV)
1a	0.34	0.31	**1b**	0.31	0.32
2a	0.25	0.33	**2b**	0.29	0.36
2a-iso	0.37	0.33	**2b-iso**	0.34	0.32
3a	0.29	0.27	**3b**	0.24	0.25
4a	0.21	0.29	**4b**	0.23	0.30
4a-iso	0.31	0.28	**4b-iso**	0.27	0.26
5a	0.29	0.20	**5b**	0.35	0.16
6a	0.26	0.20	**6b**	0.35	0.22

Similar trends are also found for the series of compounds **1b**−**6b** containing oxazole units (Table 2). Moreover, the reorganization energies for electrons of **1b**−**6b** are comparable to those of **1a**−**6a**, respectively. As shown above, their HOMO and LUMO levels of energy are very close together. As a consequence, all of the compounds considered here are expected to be good materials for n-type organic semiconductors.

3.4. Charge Transport Characteristics. An examination of the intermolecular transport behaviors of charge carriers requires parameters of the dimers of the molecules in different packing motifs. Due to lack of relevant experimental results, only molecules **1a**, **2a**, **2a-iso**, and **3a**, whose crystal structures were experimentally known, will be examined. Additionally, we

dx.doi.org/10.1021/jp500899k | J. Phys. Chem. A 2014, 118, 3335−3343

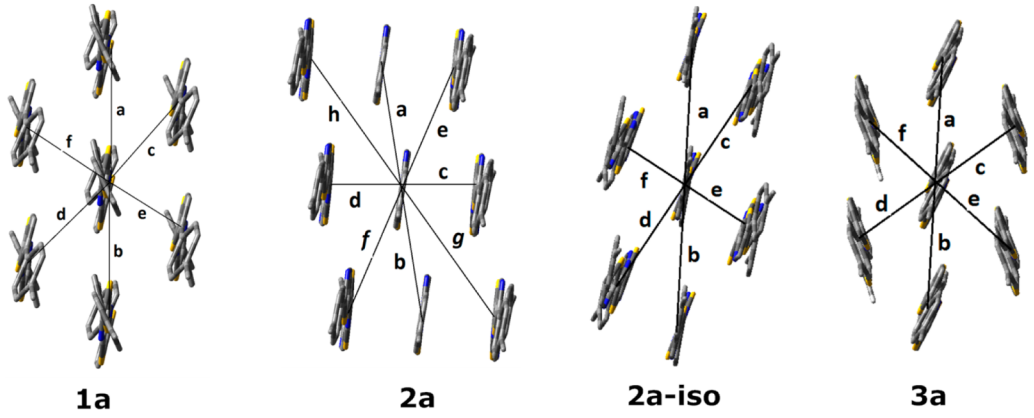

Figure 3. X-ray structures (refs 14, 15, and 17) and charge transport paths of compounds **1a**, **2a**, **2a-iso**, and **3a**. Hydrogen and fluorine atoms are removed. The X-ray structure of **3a** was refined as compared to that reported in ref 17.

only emphasized the transport characteristics for electron because, as mentioned above, these compounds are probed to be good materials for n-type semiconductors. The corresponding dimers are constructed using experimental parameters of their crystalline lattices. Several charge transport pathways of compounds are shown in Figure 3 and Figure S2 of the Supporting Information.

Our computed results point out that intermolecular charge transports of these compounds mainly occur among molecules in the same molecular layer. Intermolecular interactions between molecules in different molecular layers are in fact very small (Figure S2, Supporting Information).

It is known that the computed intermolecular transfer integrals are very sensitive to DFT functionals. Recently, Sutton et al.[56] showed that increasing amount of HF exchange in DFT functionals will increase the predicted transfer integral values in a nearly linear fashion. In the present work, we performed calculations of transfer integrals for various transport pathways of above compounds by using several functionals (PW91, B3LYP, M06,[57] BhandHLYP,[58] and M06HF[59] that contain amount of HF exchange of 0%, 20%, 27%, 50%, and 100%, respectively). Our results in Table 3 are consistent with the previous reports that the transfer integral values of compounds are largest when functional M06-HF (with percent of HF exchange of 100%) is used. The smallest values are obtained when pure functional PW91 is used. However, we would note that the effect of HF exchange (the actual fraction) also depends on the compounds considered and is not always in linear motif as previously shown. Interestingly, it can be observed that the transfer integrals of pathways **c** and **e** in compound **1** are much larger than those of **d** and **f**, respectively, although their intermolecular distances are approximate. This can be understood from the fact that arrangements of thiophene groups in these dimers differ from each other. As shown in Figure S4 (Supporting Information), in dimers **c** and **e** the two thiophene groups in two monomers can be regarded as having a head-to-tail configuration, whereas they are rather in a head-to-head configuration in both dimers **d** and **f**.

While geometries of two isomers **2a** and **2a-iso** are similar, their packing motifs in X-ray structures are quite different from each other (Figure 3). For both isomers, the intermolecular electron transports are mainly carried out along four pathways, **c**, **d**, **e**, and **f**, while the remaining directions are much less effective. Interestingly, the values of transfer integrals of the isomer **2a-iso** are even larger than those of **2a**. The maximum

Table 3. Distance between Two Monomers (d, Å) and Transfer Integral (t_e, meV) in Several Charge Transport Paths of Compounds 1a, 2a, 2a-iso, and 3a

		transfer integral (meV)				
pathways	d (Å)	PW91	B3LYP	M06	BH and HLYP	M06HF
			1a			
a, b	6.05	5.03	5.58	6.67	6.12	4.90
c	5.11	43.13	48.16	48.16	53.06	57.82
d	5.68	1.09	1.77	0.54	8.30	10.88
e	4.26	70.34	83.54	84.08	103.68	128.57
f	5.32	4.76	7.35	7.48	13.88	20.41
			2a			
a, b	5.914	8.98	10.61	11.16	12.93	13.20
c, d	3.982	26.80	33.74	30.34	42.04	42.72
e, f	6.333	14.42	16.60	16.74	20.54	23.40
g, h	7.769	4.49	7.21	7.48	11.16	14.42
			2a-iso			
a, b	8.43	1.63	1.90	1.63	2.18	2.18
c, d	5.86	26.67	29.39	30.07	32.79	34.15
e, f	4.665	51.02	60.95	59.05	76.06	98.51
			3a			
a, b	6	27.48	32.93	32.52	40.68	46.12
c, d, e, f	4.728	120.82	119.59	110.48	126.13	143.00

value of transfer integral for **2a-iso** attains a value of 98.51 meV (at level of theory M06-HF), which is significantly larger than that of 42.72 meV found for **2a**.

On the other hand, the compound **3a** exhibits the packing structure of herringbone type, rather than π-stacking structures of compounds **1a**, **2a**, and **2a-iso**, whereas the compounds **4a** and **4a-iso** were suggested as amorphous or distorted structures.[17] Our computed results show that the charge transport for electron of **3a** is mainly carried out along transport pathways **c**, **d**, **e**, and **f** in face-to-edge motif (t_e = 143.0 meV). The transfer integral along pathways **a** and **b** in face-to-face motif is much lower (t_e = 46.12 meV).

The hopping drift mobility (μ) is calculated by using the Einstein relation (eq 8):

$$\mu = eD/k_BT \tag{8}$$

where e is the electronic charge and D the diffusion coefficient that is calculated from eq 9:[60,61]

dx.doi.org/10.1021/jp500899k | J. Phys. Chem. A 2014, 118, 3335−3343

Table 4. Hopping Rate (K, s^{-1}) for Electron in Several Charge Transport Pathways and Mobility (μ, $cm^2\ V^{-1}\ s^{-1}$) of Compounds 1a, 2a, 2a-iso, and 3a

	PW91	B3LYP	M06	BH and HLYP	M06-HF
			Compound **1a**		
hopping rate $K \times 10^{-12}$ (s^{-1})					
a	0.027	0.033	0.047	0.039	0.025
b	0.027	0.033	0.047	0.039	0.025
c	0.001	0.003	0.000	0.072	0.125
d	1.958	2.441	2.441	2.963	3.519
e	0.024	0.057	0.059	0.203	0.438
f	5.207	7.344	7.440	11.311	17.397
mobility ($cm^2\ V^{-1}\ s^{-1}$)	0.53×10^{-1}	0.74×10^{-1}	0.75×10^{-1}	1.13×10^{-1}	1.76×10^{-1}
			Compound **2a**		
hopping rate $K \times 10^{-12}$ (s^{-1})					
a, b	0.238	0.332	0.367	0.492	0.513
c, d	2.117	3.356	2.713	5.210	5.380
e, f	0.613	0.812	0.825	1.244	1.614
g, h	0.059	0.153	0.165	0.367	0.613
mobility ($cm^2\ V^{-1}\ s^{-1}$)	0.19×10^{-1}	0.29×10^{-1}	0.24×10^{-1}	0.45×10^{-1}	0.48×10^{-1}
			Compound **2a-iso**		
hopping rate $K \times 10^{-12}$ (s^{-1})					
a, b	0.002	0.003	0.002	0.004	0.004
c, d	0.536	0.651	0.681	0.810	0.879
e, f	1.961	2.799	2.627	4.357	7.309
mobility ($cm^2\ V^{-1}\ s^{-1}$)	0.24×10^{-1}	0.35×10^{-1}	0.33×10^{-1}	0.55×10^{-1}	0.94×10^{-1}
			Compound **3a**		
hopping rate $K \times 10^{-12}$ (s^{-1})					
a, b	1.400	2.010	1.960	3.068	3.944
c, d	27.063	26.517	22.628	29.492	37.910
e, f	27.063	26.517	22.628	29.492	37.910
mobility ($cm^2\ V^{-1}\ s^{-1}$)	3.84×10^{-1}	3.72×10^{-1}	3.17×10^{-1}	4.10×10^{-1}	5.27×10^{-1}

$$D = (1/2n) \sum_i d_i^2 K_i P_i \quad (9)$$

where n is the dimensionality ($n = 3$), d_i the center of mass distance to neighbor i, K_i the hopping rate which is calculated using eq 1, and P_i the relative probability for charge carrier to an ith neighbor ($P_i = K_i/\sum_i K_i$).

The electron hopping rate for several transport pathways of compounds and their drift mobility are given in Table 4. The mobility of **1a** varies in the range of 0.53×10^{-1} to 1.76×10^{-1} $cm^2\ V^{-1}\ s^{-1}$. These values are in good agreement with the experimental value of 1.2×10^{-1} $cm^2\ V^{-1}\ s^{-1}$ (obtained at substrate temperature of 25 °C).[15] The computed mobility of compound **3a** is in the range of 3.84×10^{-1} to 5.27×10^{-1} $cm^2\ V^{-1}\ s^{-1}$, which are somewhat higher than the experimental values of 1.0×10^{-1} to 2.4×10^{-1} $cm^2\ V^{-1}\ s^{-1}$.[14] At substrate temperature of 20 °C, the earlier experimental study showed that the electron mobility of compound **2a** is 0.03×10^{-1} to 3.8×10^{-1} $cm^2\ V^{-1}\ s^{-1}$,[17] which are comparable to our theoretical values of 0.19×10^{-1} to 0.48×10^{-1} $cm^2\ V^{-1}\ s^{-1}$. Although the electron mobility of **2a-iso** is equal to 0.003×10^{-1} $cm^2\ V^{-1}\ s^{-1}$ in a previous experimental report,[14] our theoretical value is much larger and varies in the range of 0.24×10^{-1} to 0.94×10^{-1} $cm^2\ V^{-1}\ s^{-1}$. This value is even larger than the corresponding value of compound **2a**. The reason for this discrepancy comes from the much larger transfer integrals of **2a-iso** as compared to those of **2a**. We expect that a re-examination of X-ray structures of two these compounds could be carried out in either theoretical or experimental studies in the near future.

4. CONCLUDING REMARKS

In the present work, we designed and investigated the characteristics of molecular structure and charge transport properties of some new n-type organic semiconductors containing thiazole (**1a**−**6a**) and oxazole (**1b**−**6b**) frameworks and terminal groups of trifluoromethylphenyl using density functional theory (DFT) methods. The main points emerge as follows:

(i) The HOMO and LUMO energy levels of compounds considered are decreased when thiophene and furan moieties of compounds **1a**−**2a** and **1b**−**2b** are replaced by thiazole (of compounds **3a**−**4a**) and oxazole (of compounds **3b**−**4b**) moieties, respectively. The same trend was observed when benzo[1,2-*d*:4,5-*d*′]bisthiazole groups are replaced with benzo[1,2-*d*:4,5-*d*′]bisthiazole-4,8-diones. The effect of the dione on LUMO energy levels of oxazole analogues is larger than that of the thiazole counterparts. The LUMO energy levels of compounds **5b** and **6b** are systemically lower than those of **5a** and **6a**, respectively. The LUMO values of **1b**−**4b** turn out to be higher than those of **1a**−**4a**, respectively.

(ii) The reorganization energies for electron of compounds are in the range of 0.21−0.37 eV, which is comparable to the value of 0.25 eV of well-known n-type semiconductors such as perfluoropentacene.

(iii) Replacement of the core thiazolelothiazole unit of compounds **1a** and **2a** by the larger core units of **3a** and **4a** invariably decreases their reorganization energies for electron (λ_e).

dx.doi.org/10.1021/jp500899k | J. Phys. Chem. A 2014, 118, 3335−3343

(iv) The λ_e values of compounds containing thiazole (**2a**, **4a**, and **6a**) are predicted to be smaller than those of compounds containing thiophene (**1a**, **3a**, and **5a**), respectively.

(v) No clear trend can be emphasized when replacing benzene rings of compounds **3a** and **4a** by quinone rings of compounds **5a** and **6a**. The λ_e values of **5a** and **6a** are only slightly larger. A similar trend is also found for compounds containing oxazole **1b**−**6b**.

(vi) The intermolecular charge transports in solid state of these compounds mainly occur among molecules in the same molecular layer, whereas intermolecular interactions between molecules in different molecular layers are very small.

(vii) The transfer integral of dimers considerably depends on the amount of HF exchange of the functionals used, but there is no linear correlation.

In summary, besides the molecules **1a**−**4a** that were experimentally reported, the remaining molecules designed in the present work can be proposed as very good candidates for n-type organic semiconducting materials with small reorganization energies for electron and low LUMO energy levels.

■ ASSOCIATED CONTENT

Supporting Information

Shapes and Cartesian coordinates of the optimized geometries of compounds **1a**−**6a** and **1b**−**6b**. The charge transport paths in solid state of compounds **1a**, **2a**, and **2a-iso**. Shapes of molecules **2a**, **2a-iso**, **4a**, and **4a-iso** in both neutral and anionic states. Direction of dimers **a**, **b**, **c**, and **d** of compound **1a**. This material is available free of charge via the Internet at http://pubs.acs.org.

■ AUTHOR INFORMATION

Corresponding Author

*E-mail: minh.nguyen@chem.kuleuven.be. Fax: +32-16-327992.

Notes

The authors declare no competing financial interest.

■ ACKNOWLEDGMENTS

We are indebted to the KU Leuven Research Council (GOA program) for continuing support. T.B.T. is grateful to the FWO-Vlaanderen for a postdoctoral fellowship. V.T.T.H. thanks the FWO-Vlaanderen for a Ph.D. scholarship. We would like to thank Prof. Masashi Mamada, Yamagata University, Japan, for a refined X-ray structure of compound **3a** and valuable discussion.

■ REFERENCES

(1) Dimitrakopoulos, C. D.; Malenfant, P. R. L. Organic Thin Film Transistors for Large Area Electronics. *Adv. Mater.* **2002**, *14*, 99−117.

(2) Katz, H. E.; Bao, Z. The Physical Chemistry of Organic Field Effect Transistors. *J. Phys. Chem. B* **2000**, *104*, 671−678.

(3) Nelson, S. F.; Lin, Y. Y.; Gundlach, D. J.; Jackson, T. N. Temperature-independent Transport in High-mobility Pentacene Transistors. *Appl. Phys. Lett.* **1998**, *72*, 1854−1856.

(4) Sundar, V. C.; Zaumseil, J.; Podzorov, V.; Menard, E.; Willett, R. L.; Someya, T.; Gershenson, M. E.; Rogers, J. A. Elastomeric Transistor Stamps: Reversible Probing of Charge Transport in Organic Crystals. *Science* **2004**, *303*, 1644−1646.

(5) Podzorov, V.; Menard, E.; Borissov, A.; Kiryukhin, V.; Rogers, J. A.; Gershenson, M. E. Intrinsic Charge Transport on the Surface of Organic Semiconductors. *Phys. Rev. Lett.* **2004**, *93*, 86602/1−86602/4.

(6) Kanicki, J.; Libsch, F. R.; Griffith, J.; Polastre, R. Performance of Thin Hydrogenated Amorphous Silicon Thin-film Transistors. *J. Appl. Phys.* **1991**, *69*, 2339−2345.

(7) Chesterfield, R. J.; Newman, C. R.; Pappenfls, T. M.; Ewbank, P. C.; Haukaas, M. H.; Mann, K. R.; Miller, L. L.; Frisbie, C. D. High Electron Mobility and Ambipolar Transport in Organic Thin-Film Transistors Based on a π-Stacking Quinoidal Terthiophene. *Adv. Mater.* **2003**, *15*, 1278−1282.

(8) (a) Sakamoto, Y.; Suzuki, T.; Kobayashi, M.; Gao, Y.; Fukai, Y.; Inoue, Y.; Sato, F.; Tokito, S. Perfluoropentacene: High-Performance, p-n Junctionsand Complementary Circuits with Pentacene. *J. Am. Chem. Soc.* **2004**, *126*, 8138−8140. (b) Mushrush, M.; Facchetti, A.; Lefenfeld, M.; Katz, H. E.; Marks, T. J. Easily Processable Phenylene-thiophene-based Organic Field-effect Transistors and Solution-fabricated Nonvolatile Transistor Memory Elements. *J. Am. Chem. Soc.* **2003**, *125*, 9414−9423. (c) Yoon, M. H.; Di Benedetto, S. A.; Facchetti, A.; Marks, T. J. Organic Thin-Film Transistors Based on Carbonyl-Functionalized Quaterthiophenes: High Mobility N-Channel Semiconductors and Ambipolar Transport. *J. Am. Chem. Soc.* **2005**, *127*, 1348−1349.

(9) Wang, C.; Dong, H.; Hu, W.; Liu, Y.; Zhu, D. Semiconducting π-Conjugated Systems in Field-Effect Transistors: A Material Odyssey of Organic Electronics. *Chem. Rev.* **2012**, *112*, 2208−2267.

(10) Mishra, A.; Ma, C.-Q.; Bauerle, P. Functional Oligothiophenes: Molecular Design for Multidimensional Nanoarchitectures and Their Applications. *Chem. Rev.* **2009**, *109*, 1141−1276.

(11) Osaka, I.; Takimiya, K.; McCullough, R. D. Benzobisthiazole-Based Semiconducting Copolymers Showing Excellent Environmental Stability in High-Humidity Air. *Adv. Mater.* **2010**, *22*, 4993−4997.

(12) Bevk, D.; Marin, L.; Lutsen, L.; Vanderzande, D.; Maes, W. Thiazolo[5,4-d]thiazoles−Promising Building Blocks in the Synthesis of Semiconductors for Plastic Electronics. *RSC Adv.* **2013**, *3*, 11418−11431.

(13) Ando, S.; Nishida, J.; Tada, H.; Inoue, Y.; Tokito, S.; Yamashita, Y. High Performance n-Type Organic Field-Effect Transistors Based on π-Electronic Systems with Trifluoromethylphenyl Groups. *J. Am. Chem. Soc.* **2005**, *127*, 5336−5337.

(14) Mamada, M.; Nishida, J.-I.; Kumaki, D.; Tokito, S.; Yamashita, Y. n-Type Organic Field-Effect Transistors with High Electron Mobilities Based on Thiazole−Thiazolothiazole Conjugated Molecules. *Chem. Mater.* **2007**, *19*, 5404−5409.

(15) Ando, S.; Nishida, J.; Tada, H.; Inoue, Y.; Tokito, S.; Yamashita, Y. High Performance n-Type Organic Field-Effect Transistors Based on π-Electronic Systems with Trifluoromethylphenyl Groups. *J. Am. Chem. Soc.* **2005**, *127*, 5336−5337.

(16) Kumaki, D.; Ando, S.; Shimono, S.; Yamashita, Y. Significant Improvement of Electron Mobility in Organic Thin-film Transistors based on Thiazolothiazole Derivative by Employing Self-assembled Monolayer. *Appl. Phys. Lett.* **2007**, *90*, 053506/01−03.

(17) Mamada, M.; Nishida, J.-I.; Tokito, S.; Yamashita, Y. Preparation, Characterization and Field-effect Transistor Performance of Benzo[1,2-d:4,5-d′]bisthiazole Derivatives. *Chem. Lett.* **2008**, *37*, 766−767.

(18) Nelsen, S. F.; Blomgren, F. Estimation of Electron Transfer Parameters from AM1 Calculations. *J. Org. Chem.* **2001**, *66*, 6551−6559.

(19) Nelsen, S. F.; Trieberi, D. A.; Ismagilov, R. F.; Teki, Y. Solvent Effects on Charge Transfer Bands of Nitrogen-Centered Intervalence Compounds. *J. Am. Chem. Soc.* **2001**, *123*, 5684−5694.

(20) Malagoli, M.; Brédas, J. L. Density Functional Theory Study of the Geometric Structure and Energetics of Triphenylamine-based Hole-transporting Molecules. *Chem. Phys. Lett.* **2000**, *327*, 13−17.

(21) Sakanoue, K.; Motoda, M.; Sugimoto, M.; Sakaki, S. A Molecular Orbital Study on the Hole Transport Property of Organic Amine Compounds. *J. Phys. Chem. A* **1999**, *103*, 5551−5556.

(22) Li, X. Y.; Tong, J.; He, F. C. Ab initio Calculation for Inner Reorganization Energy of Gas-Phase Electron Transfer in Organic Molecule−ion Systems. *Chem. Phys.* **2000**, *260*, 283−294.
(23) Marcus, R. A.; Sutin, N. Electron Transfers in Chemistry and Biology. *Biochim. Biophys. Acta* **1985**, *811*, 265−322.
(24) Marcus, R. A. Electron Transfer Reactions in Chemistry. Theory and Experiment. *Rev. Mod. Phys.* **1993**, *65*, 599−610.
(25) Troisi, A.; Orlandi, G. The Hole Transfer in DNA: Calculation of Electron Coupling Between Close Bases. *Chem. Phys. Lett.* **2001**, *344*, 509−518.
(26) Troisi, A.; Orlandi, G. Dynamics of the Intermolecular Transfer Integral in Crystalline Organic Semiconductors. *J. Phys. Chem. A* **2006**, *110*, 4065−4070.
(27) Yin, S.; Yi, Y.; Li, Q.; Yu, G.; Liu, Y.; Shuai, Z. G. Balanced Carrier Transports of Electrons and Holes in Silole-Based CompoundsA Theoretical Study. *J. Phys. Chem. A* **2006**, *110*, 7138−7143.
(28) Perdew, J. P.; Chevary, J. A.; Vosko, S. H.; Jackson, K. A.; Pederson, M. R.; Singh, D. J.; Fiolhais, C. Atoms, Molecules, Solids, and Surfaces: Applications of the Generalized Gradient Approximation for Exchange and Correlation. *Phys. Rev. B* **1992**, *46*, 6671−6687.
(29) Perdew, J. P.; Burke, K.; Wang, Y. Generalized Gradient Approximation for the Exchange-Correlation Hole of a Many-electron System. *Phys. Rev. B* **1996**, *54*, 16533−16539.
(30) Huang, J.; Kertesz, M. Intermolecular Transfer Integrals for Organic Molecular Materials: Can Basis Set Convergence Be Achieved? *Chem. Phys. Lett.* **2004**, *390*, 110−115.
(31) Li, H.; Zheng, R.; Shi, Q. Theoretical Study of Charge Carrier Transport in Organic Semiconductors of Tetrathiafulvalene Derivatives. *J. Phys. Chem. C* **2012**, *116*, 11886−11894.
(32) Yang, X.; Wang, L.; Wang, C.; Long, W.; Shuai, Z. Influences of Crystal Structures and Molecular Sizes on the Charge Mobility of Organic Semiconductors: Oligothiophenes. *Chem. Mater.* **2008**, *20*, 3205−3211.
(33) Nan, G.; Yang, X.; Wang, L.; Shuai, Z.; Zhao, Y. Nuclear Tunneling Effects of Charge Transport in Rubrene, Tetracene, and Pentacene. *Phys. Rev. B* **2009**, *79*, 115203/1−9.
(34) Yang, X.; Li, Q.; Shuai, Z. Theoretical Modelling of Carrier Transports in Molecular Semiconductors: Molecular Design of Triphenylamine Dimer Systems. *Nanotechnology* **2007**, *18*, 424029/1−6.
(35) (a) Huong, V. T. T.; Tai, T. B.; Nguyen, M. T. The π-Conjugated P-Flowers $C_{16}(PH)_8$ and $C_{16}(PF)_8$ are Potential Materials for Organic n-type Semiconductors. *Phys. Chem. Chem. Phys.* **2012**, *14*, 14832−14841. (b) Huong, V. T. T; Huyen, N. T.; Tai, T. B.; Nguyen, M. T. π-Conjugated Molecules Containing Naphtho[2,3-b]thiophene and Their Derivatives: Theoretical Design for Organic Semiconductors. *J. Phys. Chem. C* **2013**, *117*, 10175−10184. (c) Tai, T. B.; Huong, V. T. T.; Nguyen, M. T. Design of Aromatic Heteropolycyclics Containing Borole Frameworks. *Chem. Commun.* **2013**, *49*, 11548−11550.
(36) Tang, X.; Liao, Y.; Gao, H.; Geng, Y.; Su, Z. Theoretical Study of The Bridging Effect on the Charge Carrier Transport Properties of Cyclooctatetrathiophene and Its Derivatives. *J. Mater. Chem.* **2012**, *22*, 6907−6918.
(37) Chen, X.; Zou, L.; Gou, J.; Ren, A. An Efficient Strategy for Designing n-type Organic Semiconductor Materials—Introducing a Six-membered Imide Ring into Aromatic Diimides. *J. Mater. Chem.* **2012**, *22*, 6471−6484.
(38) Nan, G.; Li, Z. Phase Dependence of Hole Mobilities in Dibenzo-tetrathiafulvalene Crystal: A First-Principles Study. *Org. Electron.* **2012**, *13*, 1229−1236.
(39) Davis, A. P.; Fry, A. J. Experimental and Computed Absolute Redox Potentials of PolycyclicAromatic Hydrocarbons are Highly Linearly Correlated Over a Wide Range of Structures and Potentials. *J. Phys. Chem. A* **2010**, *114*, 12299−12304.
(40) Marenich, A. V.; Cramer, C. J.; Truhlar, D. G. Universal Solvation Model Based on Solute Electron Density and on a Continuum Model of the Solvent Defined by the Bulk Dielectric Constant and Atomic Surface Tensions. *J. Phys. Chem. B* **2009**, *113*, 6378−6396.
(41) Namazian, M.; Lin, C. Y.; Coote, M. L. Benchmark Calculations of Absolute Reduction Potential of Ferricinium/Ferrocene Couple in Nonaqueous Solutions. *J. Chem. Theory Comput.* **2010**, *6*, 2721−2725.
(42) Bartmess, J. E. Thermodynamics of the Electron and the Proton. *J. Phys. Chem.* **1994**, *98*, 6420−6424.
(43) Lee, C.; Yang, W.; Parr, R. G. Development of the Colle-Salvetti Correlation-Energy Formula into a Functional of the Electron Density. *Phys. Rev. B* **1988**, *37*, 785−789.
(44) Becke, A. D. Density-functional Exchange-Energy Approximation with Correct Asymptotic Behavior. *Phys. Rev. A* **1988**, *38*, 3098−3100.
(45) Stephens, P. J.; Devlin, F. J.; Chabalowski, C. F.; Frisch, M. J. Ab Initio Calculation of Vibrational Absorption and Circular Dichroism Spectra Using Density Functional Force Fields. *J. Phys. Chem.* **1994**, *98*, 11623−11627.
(46) Hariharan, P. C.; Pople, J. A. The Influence of Polarization Functions on Molecular Orbital Hydrogenation Energies. *Theor. Chim. Acta* **1973**, *28*, 213−222.
(47) Francl, M. M.; Petro, W. J.; Hehre, W. J.; Binkley, J. S.; Gordon, M. S.; DeFrees, D. J.; Pople, J. A. Self-consistent Molecular Orbital Methods. XXIII. A Polarization-Type Basis Set for Second-Row Elements. *J. Chem. Phys.* **1982**, *77*, 3654−3665.
(48) Trucks, G. W.; et al. *Gaussian 09, Revision A.02*; Gaussian, Inc.: Wallingford CT, 2009.
(49) Tai, T. B.; Huong, V. T. T.; Nguyen, M. T. Theoretical Design of π-Conjugated Heteropolycyclic Compounds Containing a Tricoordinated Boron Center. *J. Phys. Chem. C* **2013**, *117*, 14999−15008.
(50) Chai, S.; Wen, S. H.; Huang, J. D.; Han, K. L. Density Functional Theory Study on Electron and Hole Transport Properties of Organic Pentacene Derivatives with Electron-Withdrawing Substituent. *J. Comput. Chem.* **2011**, *32*, 3218−3225.
(51) (a) Gahungu, G.; Zhang, B.; Zhang, J. Design of Tetrathiafulvalene-Based Phosphazenes Combininga Good Electron-Donor Capacity and Possible Inclusion Adduct Formation (Part II). *J. Phys. Chem. C* **2007**, *111*, 4838−4846. (b) Gahungu, G.; Zhang, J.; Barancira, T. Charge Transport Parameters and Structural and Electronic Properties of Octathio[8]circulene and Its Plate-like Derivatives. *J. Phys. Chem. A* **2009**, *113*, 255−262. (c) Gahungu, G.; Zhang, J. Shedding Light on Octathio[8]circulene and Some of Its Plate-like Derivatives. *Phys. Chem. Chem. Phys.* **2008**, *10*, 1743−1747.
(52) Wartelle, C.; Viruela, R.; Viruela, P. M.; Sauvage, F. X.; Salle, M.; Orti, E.; Levillain, E.; Le Derf, F. First Signals of Electrochemically Oxidized Species of TTF and TTM-TTF: A Study by in Situ Spectroelectrochemical FTIR and DFT Calculations. *Phys. Chem. Chem. Phys.* **2003**, *5*, 4672−4679.
(53) Kim, E. G.; Coropceanu, V.; Gruhn, N. E.; Sanchez-Carrera, R. S.; Snoeberger, R.; A.J. Matzger, A. J.; Bredas, J. L. Charge Transport Parameters of the Pentathienoacene Crystal. *J. Am. Chem. Soc.* **2007**, *129*, 13072−13081.
(54) Bromley, S. T.; Mas-Torrent, M.; Hadley, P.; Rovira, C. Importance of Intermolecular Interactions in Assessing Hopping Mobilities in Organic Field Effect Transistors:Pentacene versus Dithiophene-tetrathiafulvalene. *J. Am. Chem. Soc.* **2004**, *126*, 6544−6545.
(55) Marenich, A. V.; Cramer, C. J.; Truhlar, D. G. Universal Solvation Model Based on Solute Electron Density and on a Continuum Model of the Solvent Defined by the Bulk Dielectric Constant and Atomic Surface Tensions. *J. Phys. Chem. B* **2009**, *113*, 6378−6396.
(56) Sutton, C.; Sears, J. S.; Coropceanu, V.; Bredas, J.-L. Understanding the Density Functional Dependence of DFT Calculated Electronic Couplings in Organic Semiconductors. *J. Phys. Chem. Lett.* **2013**, *4*, 919−924.
(57) Zhao, Y.; Truhlar, D. G. The M06 Suite of Density Functionals for Main Group Thermochemistry, Thermochemical Kinetics, Noncovalent Interactions, Excited States, and Transition Elements: Two New Functionals and Systematic Testing of Four M06-class

Functionals and 12 Other Functional. *Theor. Chem. Acc.* **2006**, *120*, 215−241.
(58) Becke, A. D. A New Mixing of Hartree-Fock and Local Density-Functional Theories. *J. Chem. Phys.* **1993**, *98*, 1372−1377.
(59) Zhao, Y.; Truhlar, D. G. Density Functional for Spectroscopy: No Long-Range Self-Interaction Error, Good Performance for Rydberg and Charge-Transfer States, and Better Performance on Average than B3LYP for Ground States. *J. Phys. Chem. A* **2006**, *110*, 13126−13130.
(60) Schein, L. B.; McGhie, A. R. Band-Hopping Mobility Transition in Naphthalene and Deuterated Naphthalene. *Phys. Rev. B* **1979**, *20*, 1631−1639.
(61) Deng, W. Q.; Goddard, W. A. Predictions of Hole Mobilities in Oligoacene Organic Semiconductors from Quantum Mechanical Calculations. *J. Phys. Chem. B* **2004**, *108*, 8614−8621.